Laminin- and basement membrane-polycaprolactone blend nanofibers as a scaffold for regenerative medicine

Rebekah A. Neal,
University of Virginia Department of Biomedical Engineering, Charlottesville, VA 22903, USA

Steven M. Lenz,
University of Virginia Department of Biomedical Engineering, Charlottesville, VA 22903, USA

Tiffany Wang,
Georgia Institute of Technology and Emory University Department of Biomedical Engineering, Atlanta, Georgia 30332, USA

Daniel Abebayehu,
University of Virginia Department of Biomedical Engineering, Charlottesville, VA 22903, USA

Benjamin P.C. Brooks,
University of Virginia Department of Biomedical Engineering, Charlottesville, VA 22903, USA

Roy C. Ogle, and
Old Dominion University School of Medical Diagnostic & Translational Sciences, Norfolk, VA 23529, USA

Edward A. Botchwey[*]
Georgia Institute of Technology and Emory University Department of Biomedical Engineering, Atlanta, Georgia 30332, USA

Abstract

Mimicking one or more components of the basement membrane (BM) holds great promise for overcoming insufficiencies in tissue engineering therapies. We have electrospun laminin nanofibers (NFs) isolated from the murine Engelbreth-Holm Swarm (EHS) tumor and evaluated them as a scaffold for embryonic stem cell culture. Seeded human embryonic stem cells were found to better maintain their undifferentiated, colony environment when cultured on laminin NFs compared to laminin mats, with 75% remaining undifferentiated on NFs. Mouse embryonic stem cells cultured on 10% laminin-polycaprolactone (PCL) NFs maintained their colony formation for twice as long without passage compared to those on PCL or gelatin substrates. In addition, we have established a protocol for electrospinning reconstituted basement membrane aligned (RBM)-PCL NFs within 10° of angular deviation. Neuron-like PC12 cells show significantly greater attachment (p < 0.001) and percentage of neurite-extending cells *in vitro* on 10% RBM-PCL NFs when compared to 1% and 0% RBM-PCL NFs (p < 0.015 and p < 0.001, respectively). Together,

[*]**Corresponding author Edward A. Botchwey:** Phone: 404-385-5058, Fax: 404-894-4243, edward.botchwey@bme.gatech.edu.

these results implicate laminin- and RBM-PCL scaffolds as a promising biomimetic substrate for regenerative medicine applications.

Keywords

basement membrane; laminin; polycaprolactone; embryonic stem cells; peripheral nerve regeneration

1 Introduction

Basement membrane (BM) is a three dimensional, multifunctional, and composite material consisting primarily of type IV collagen and the glycoprotein laminin, with nidogen and perlecan functioning to crosslink the collagen and laminin networks [1]. The BM is first deposited during fetal development and provides the surface for endothelium throughout the body, lines the nervous system, and encapsulates muscle fibers. Much remains to be understood about the tissue specificity of BM and the function of the minor components within the matrix.

The complex nanotopography of this natural substrate consists of interconnected fibers and pores, with feature sizes in the 30–400nm range [1], which can be closely replicated by various techniques for creating nanofibrous structures [2]. The geometry of BM as a porous, fibrous mesh allows for its functions as structural support for the organization of cell layers, as a semipermeable barrier in the glomerulus, and as a binding site and growth factor reservoir for cell fate determination and tissue maintenance. Significant work has addressed the effect of such feature sizes and shapes on cell adhesions, shape and orientation, migration, and differentiation, and concluded that feature shape and size are indeed relevant for cell behavior [3–9], but their effects are specific to cell type, suggesting BM characteristics may vary throughout the body.

In addition to feature geometry, research has addressed the effects of various membrane components on cell fate; however, little work has interrogated the synergy of geometry and composition. In previous studies, we established that nanofibers composed of the glycoprotein laminin alone [10] or blended with synthetic polymers [11], provide sufficient BM mimetic cues to promote attachment and outgrowth in the peripheral nervous system. We have also shown that laminin-synthetic blend nanofibers promote sufficient adhesion for transplantation of photoreceptor cells, and other groups have shown the adhesive effects of type IV collagen [12–14]. Single BM-derived protein scaffolds may also serve as ideal substrates for other regenerative medicine applications, such as maintaining embryonic stem cells in an undifferentiated phenotype. An obstacle in the current standard of practice for embryonic stem cell maintenance is the production of highly immunogenic xenogenic byproducts from mouse cell feeder (MEFs) layers [15]; replacing MEFs with a defined, single or multiple component BM scaffold could overcome this challenge and prove more cost effective than using human derived feeder layers [16,17]. Prior studies in our laboratory demonstrated that reconstituted laminin I derived from the murine Engelbreth Holm Swarm (EHS) tumor had the same bioactivity as native laminin in promoting neurite outgrowth [10], suggesting its utility as a BM-mimetic substrate. In this current work, utilizing nanofibrous

laminin surfaces, we show that laminin nanofibers serve to mimic BM geometry by providing BM-scale nanotopography in addition to providing sufficient cues for maintenance of undifferentiated embryonic stem cells without the use of feeder cell layers.

While simple systems comprised of one or more BM components may be sufficient to form an idealized BM-like substrate for a specific tissue or culture, the ability to mimic both the structure and the broader composition of the *in vivo* BM may provide further advantages for recapitulating *in vivo* cell behavior and modulating cell fate. Whole BM isolated from the murine EHS tumor is almost identical in composition to native, healthy BM and as such may be used as a replacement for BM in culture [1,18,19]. In these studies, we have isolated BM from the EHS tumor and fabricated nanofibers from this reconstituted basement membrane (RBM), as well as blending RBM with polycaprolactone (PCL) to form RBM-PCL blend nanofibers. These fibers, as both RBM alone and as a composite fiber RBM-PCL, provided sufficient surface structure and composition to both maintain mouse ES cells in an undifferentiated state and to drive outgrowth of peripheral neuron-like cells.

Thus, in order to manipulate BM characteristics, we have developed an extracellular matrix protein-based system that can be readily adapted to the requirements of a specific site for tissue engineered applications. Both laminin- and BM-blend nanofibers have feature sizes and shapes comparable to native extracellular matrix. In this work we focused on two applications to validate the bioactivity of our biomaterial platform: embryonic stem cell culture and peripheral nerve repair. Specifically, we investigated laminin-blend nanofibers to replace feeder layers for embryonic stem cell culture, as well as whole BM-blend nanofibers to enhance peripheral nerve regeneration.

2 Materials and Methods

2.1 Laminin isolation

Laminin I was isolated from EHS tumor according to previously established protocols [20,21]. Throughout the isolation, all materials, equipment, and reagents were maintained at 4°C to prevent denaturation of the protein components. The protocol described is for a 100g tumor; values were adjusted depending upon the available tumor mass. Briefly, 100g frozen EHS sarcoma was thawed in 3.4M NaCl buffer for 1 hour and then homogenized to disperse the tissue. The homogenate was centrifuged and the residue was extracted overnight in 0.5M NaCl. After additional centrifugation at $11,000 \times g$, the supernatant was collected and added to 30% NHSO4 and centrifuged again. The pellet was collected and dissolved in 0.15M NaCl then dialyzed against Tris Saline. NaCl was added to final concentration of 1.7M, stirred, then brought to 3.4M NaCl. The pellet was dissolved in Tris saline, then dialyzed against 2M urea. The resulting supernatant was applied to a DEAE cellulose column after dilution with 2M urea. Unbound protein was collected after the first filtration; then the supernatant was dialyzed against 2M urea + 0.1M NaCl to collect unbound protein. Isolated laminin was stored at −70°C. Solvents were purchased from Sigma Aldrich, St. Louis, MO.

2.2 RBM isolation

RBM was isolated according to previously established protocols [22]. Throughout the isolation, all materials, equipment, and reagents were maintained at 4°C to prevent denaturation of the protein components. The protocol described is for a 100g tumor; values were adjusted for available tumor mass. 100g frozen EHS sarcoma was thawed in 200mL 3.4M NaCl buffer for 1 hour and then homogenized. The homogenate was then centrifuged at $8,000 \times g$ and the supernatant discarded. 100mL of 2M urea buffer was added to the pellets. The mixture was homogenized to disperse and left stirring for at least 12 hours at 4°C. The homogenate was then centrifuged at $23,000 \times g$ for 20 minutes, and the supernatant was saved on ice. The pellets were then homogenized in 50mL of 2M urea buffer and centrifuged at $23,000 \times g$ for 2 minutes. The supernatants were pooled and dialyzed against at least 2 liters of Tris-buffered saline (TBS) for at least 4 hours. This dialyzation step was repeated twice more with TBS. As a modification of the standard protocol to provide dry RBM for electrospinning, RBM solution was dialyzed against water to remove salts, lyophilized to remove water, and stored protected from moisture prior to use. Solvents were purchased from Sigma Aldrich.

2.3 Electrospinning protein and polymer blends

Electrospinning was carried out as previously described [10,11]. Briefly, initial solutions were loaded into a 5 mL syringe placed in an Aladdin programmable syringe pump (World Precision Instruments, Sarasota, FL) and a positive voltage was applied (Gamma High Voltage, Ormond Beach, FL). Solution was dispensed at a specified flow rate between 0.5 and 2 mL/hr and collected across a 20 cm working distance onto either a grounded aluminum sheet for characterization or onto clean glass coverslips for cell culture. Electrospinning was stopped when all solution had been dispensed from the 5 mL syringe. Meshes for fiber morphology characterization were mounted on aluminum stubs, sputter coated with gold (BALTEC, Los Angeles, CA) and imaged using a JEOL 6400 scanning electron microscope (SEM) with Orion image processing (JOEL USA, Acworth, GA).

2.4 Characterization of fiber hydration

To characterize hydration of RBM and RBM-PCL blends, samples were hydrated using Dulbecco's Modified Eagle Medium (DMEM) at 37°C in *5%* CO2 for the specified time frame. Samples were removed and air dried, and residual liquid was removed by lyophilization. Samples were prepared for SEM as described above.

2.5 Embryonic stem cell culture

Human embryonic stem (huES16) cells (gift from Stemgent) were maintained in fully defined, feeder-free mTESR medium (Stemcell Tech, BC Canada). Media was completely changed daily. Cells were plated on 100% laminin nanofibers. On day 8, cells were fixed in 4% PFA, and stained with SSEAA-4 and DAPI (gift from Stemgent).

W4 mouse embryonic stem cells (gift from UVA) were seeded onto 10% laminin nanofibers and laminin film, 100% PCL nanofibers, and gelatin at a density of 50,000 cells per scaffold. Cells were maintained in DMEM containing high glucose, 15% fetal bovine serum, 2mM glutamine, 1% penicillin/streptomycin, 0.1mM non-essential amino acids, 1mM sodium

pyruvate, 0.1mM B-mercaptoethanol (all from Life Technologies, Carlsbad, CA) and 10^3 units/mL ESGRO/LIF (Chemicon, Billerica, MA). Media was completely changed daily. At 4 and 8 days of growth without cell passaging, cells were stained with alkaline phosphatase to distinguish between undifferentiated cells (red) and differentiated cells (yellow).

2.6 PC 12 cell and tissue culture

PC12 cells were received from ATCC (CRL-1721, Manassas, VA) and maintained in DMEM: Nutrient Mixture F12 (DMEM/F12) supplemented with 10% horse serum, 5% fetal bovine serum (FBS), and 1% penicillin-streptomycin at 37°C in 5% CO_2 (Life Technologies). To establish the benefit of RBM for cell attachment, PC12 cells were plated at 50,000 cells/cm^2 in serum-free DMEM/F12 onto coverslips covered with RBM or RBM-PCL nanofibers. After 2 hours of incubation, surfaces were washed gently with PBS to remove non-adherent cells. In order to increase counting accuracy, a calcein AM (Life Technologies) solution (10 μM) was added to the media and incubated at 37°C for 40 minutes. The calcein AM solution was then washed off the surfaces and the cells were imaged using an upright Zeiss Axioskop 2 (Zeiss, Germany). The cell-covered area of each image was quantified using the ImageJ threshold function, and the diameter of at least 30 cells per image was measured using ImageJ's measurement tool. From this analysis, mean cell diameter and area of cell coverage were used to calculate the number of cells per field of view.

Neurite extension studies were also performed on RBM and RBM-PCL blend meshes. For these studies, nanofiber meshes were sterilized using ethanol washing, and PC12 cells were plated at an initial density of 20,000 cells/cm^2 in serum-free DMEM/F12. Cells were allowed to attach for 2 hours before nerve growth factor (NGF, BD Biosciences, San Jose, California) was added to a final concentration of 50ng/mL. Media were replaced after 2 days. After 5 days in culture, cells were fixed in 4% paraformaldehyde and imaged using a Zeiss Observer inverted microscope (Zeiss). Images were analyzed to yield process length and number of processes per cell. A cell was considered to be a process-extending cell if it had an extension greater than twice the diameter of the cell body. Using at least 7 fields of view, the analysis for neurite extension was characterized as the mean percentage of cells extending neurites per field of view. Neurite length was measured from the edge of the cell body to the tip of the process.

2.7 Dorsal root ganglia isolation and culture

Dorsal root ganglia (DRG) were isolated for culture from neonatal FVB/N or wild type C57/Bl6 mice in accordance with protocols approved by the Institutional Animal Care and Use Committee at the University of Virginia. DRG were gently lifted from the exposed spinal column, and fine forceps were used to mechanically disrupt capsules surrounding the DRG. DRG were grown in on nanofiber meshes in growth medium consisting of Ultraculture, with or without 10% FBS, supplemented with up to 100ng/mL nerve growth factor (NGF) as a growth stimulant. To dissociate DRG into primary neurons, freshly isolated DRG were incubated at 0.25% trypsin for 30–45 minutes at 37°C. Trypsin was removed and neurons were dissociated by repeated pipetting through decreasing sizes of

fire-polished glass pipettes. When a single cell suspension was attained, the neurons were plated on nanofiber meshes in growth medium supplemented with up to 100ng/mL NGF.

2.8 Statistical Analysis

Where appropriate, data were analyzed using Student's t-test or a one-way ANOVA with Tukey's post hoc analysis. Significance was asserted at $\alpha = 0.05$.

3 Results

3.1 Laminin nanofibers maintain stem cell quiescence

Standard electrospinning methods were employed to generate nanofibers composed of 100% laminin, 100% PCL and composite fibers of 10% laminin 90% PCL. In previous studies using the same polymer blends, Fourier transform infrared spectrometry confirmed the presence of both laminin and PCL within the blended nanofibers [11]. In those studies and the ones described here, we show nanofibers fabricated from laminin and PCL blended in solution prior to electrospinning maintain tensile properties and degradation profile of PCL alone [11]. Here, we further characterize these nanofibers using atomic force microscopy and transmission electron microscopy to show that the blended laminin-PCL nanofibers display no observable structural differences when compared to PCL nanofibers (Figure 1A, 1B). Together, these data suggest that blending laminin with PCL generates nanofibers that preserve the structural properties of PCL while displaying laminin content for enhanced cellular interaction.

To assess the bioactivity of these nanofiber scaffolds, we examined their ability to maintain embryonic stem cells in undifferentiated states. Since ES cell colony formation is necessary for continued quiescence, we studied mouse ES cell colonies cultured on 10% laminin-PCL nanofibers and PCL nanofibers, with a gelatin control (Figure 1C). After 4 days *in vitro* (DIV) without passaging, ES cells on gelatin begin to lose their colony morphology. After 8 DIV without passaging, only ES cells on laminin nanofibers maintained their colony formation, while cells on PCL, blended laminin-PCL, and gelatin begin to differentiate, as indicated by changes in alkaline phosphatase staining, and a loss of the round undifferentiated colony morphology. These results demonstrate the potential for laminin nanofibers to improve the translatability of clinical stem cell therapies through maintained pluripotency for longer durations between cell passages.

Following the observation that these nanofiber scaffolds successfully maintained stemness in mouse ES cells, we asked if these nanofibers would have the same effect on human embryonic stem cells. huES16 cells were cultured on laminin nanofibers and laminin films for 7 DIV without passaging (Figure 2A). Scanning electron micrographs show huES cells maintaining an undifferentiated state when cultured on laminin nanofibers. Counting of huES16 cells stained for the stemness marker SSEA4 showed that approximately 75% of huES16 cells cultured on laminin remained undifferentiated (Figure 2B–C).

3.2 Basement membrane-polycaprolactone nanofibers promote peripheral nerve regeneration

Utilizing standard electrospinning protocols and solvents, we successfully fabricated RBM nanofibers with varying fiber diameters and mesh morphology (Figure 3A–C). Mean nanofiber diameters ranged from 127nm to 219nm, with the smallest mean diameters found using the highest initial concentration (3% w/v) and the lowest flow rate (0.5mL/hr). Fiber diameters measured from these meshes ranged from 31nm to 780nm, with a median fiber diameter of 132nm. We found initial concentration to have a greater effect on resulting mesh morphology than flow rate (Figure 3B–C).

To ensure hydration and dissolution in aqueous media would not be a concern for these nanofibers as it can be for other protein nanofibers [23], we examined mesh morphology after up to 2 days in standard culture conditions (Figure 3D). Though fibers did experience swelling, the morphology change occurred within the first 15 minutes of hydration and that structure was maintained throughout the duration of the study, with no further increase in swelling. In addition, the fibrous morphology remained on the nanoscale, with mean hydrated diameters around 150nm.

While RBM nanofibers clearly maintain the geometry of basement membrane components, the isolation process is difficult and expensive. Therefore, to decrease cost and increase ease of use, we undertook to blend RBM with the synthetic polymer PCL. 10% RBM incorporation was determined to be an appropriate upper limit based on previous work [11,12], where we showed 10% laminin incorporation promoted comparable cell attachment and neurite extension length to 100% laminin substrates. We successfully fabricated blended nanofibers containing 1% or 10% RBM by weight, and were able to modify parameters to maintain consistent mean fiber diameters, regardless of the amount of RBM added to the mesh. Mean fiber diameters ranged from 135 to 145nm.

The utility of RBM and RBM-blend nanofibers as substrates are dependent on their ability to promote cell attachment and growth. To assess this ability, we quantified PC12 cell attachment to varying concentrations of RBM-PCL blend nanofibers (Figure 4A). Cell attachment on 1% RBM-PCL and 10% RBM-PCL nanofibers was found to be significantly greater than attachment on PCL nanofibers ($p < 0.001$).

While cell adhesion is a desirable property of most scaffolds used in regenerative medicine, successful attachment alone may not guarantee the success of a material. To further explore the value of RBM-PCL blend nanofiber meshes as a material to support peripheral nerve regeneration, we investigated the ability of these meshes to promote neurite outgrowth from both PC12 cells (Figure 4B) and primary neurons dissociated from murine DRG (Figure 4C). 10% RBM-PCL promoted a significantly greater percentage of neurite extending cells than PCL alone and 1% RBM-PCL blends ($p < 0.001$ and $p < 0.015$, respectively). Additionally, the 1% RBM-PCL substrate promoted a significantly greater fraction of neurite extending cells than pure PCL ($p < 0.001$). Together, these results suggest that RBM incorporation in PCL nanofiber meshes induces neurite extension.

Since RBM-PCL blends promote neurite extension from neurons and neuron-like cells, the next logical step is to orient this outgrowth so that we may engineer directionality into our regenerating nervous tissue. To that end, we fabricated aligned RBM-PCL blend nanofibers using the insulating gap method described previously by our group and others (Figure 5A–B) [12,24–28]. 10% RBM-PCL and 100% PCL nanofibers display mean angular deviations within 6° of the axis of alignment (Figure 5C). Aligned 10% RBM-PCL nanofibers and 100% PCL nanofibers had mean fiber diameters of approximately 200nm and 300nm, respectively, which both fall within the 30–400nm range typically observed in native BM (Figure 5D). Culture on 10% RBM, 90% PCL substrates yielded a significantly greater percentage of neurite extending cells than culture on 100% PCL substrates (p < 0.01), suggesting that aligned substrate morphology plays a critical role in guiding and outgrowth of peripheral neurons (Figure 6).

4 Discussion

The studies outlined here illustrate the utility of substrates composed of BM components such as RBM or laminin with nanofibrous topography as suitable BM-mimetic surfaces for cell culture. We demonstrated the ability of laminin-PCL blend nanofibers to better maintain human and mouse embryonic stem cell pluripotency compared to other protein-polymer and synthetic polymer only substrates. Widespread regulatory approval of stem cell use in clinical therapy is still elusive due to the presence of xenogenic factors in the culture environment generated by the murine cell feeder layer that is necessary to support the pluripotency of stem cells. A protein-based substrate has the potential to remove those xenogenic byproducts. This work helps lay the foundation for the use of isolated and reconstituted protein as sufficient to perform the function of the previously used murine cell feeder layer. While the protein used here is still murine, the absence of the xenogenic cells and their secreted factors is an improvement over feeder layer-dependent cultures. In addition, human ES cells can be maintained on recombinant laminin-511 [29], suggesting that as recombinant laminin becomes more readily available, it could replace murine-isolated laminin in these substrates. A secondary advantage of culture on laminin-or RBM-composite nanofiber meshes is an increase in time between cell passaging. Currently, the requirement for frequent cell passage to maintain a stem cell culture makes large-scale stem cell supplies difficult; a potential increase in duration between cell passaging makes large scale culture at point-of-care more feasible.

Nevertheless, should BM-derived protein scaffolds provide minimal clinical improvements over current ES culture practices, there remains an alternate benefit of nanofibers; namely, the ability to encourage differentiation down a specific lineage. PCL nanofibers have been shown to enhance the differentiation of mouse ES cells down a neural lineage [30–32]. Xie *et al.* showed decreased astrocytic differentiation on aligned substrates compared to random nanofibers, and specifically using unaligned laminin peptide-derived nanofibers showed less astrocytic differentiation of ES cell cultures [30]. PCL nanofibers have also been shown to promote differentiation of mesenchymal stem cells down a neuronal lineage under neuron growth media, but were shown to maintain a fibroblastic phenotype under traditional growth media [33]. In our laboratory, we have previously demonstrated the ability to form both random and aligned meshes of laminin-PCL blends as well as pure PCL [11], and here we

have demonstrated the ability to align RBM-PCL blends. With the ability to create the unique combination of nanofibers that are aligned and contain bioactive laminin, these substrates may indeed prove to be significantly more effective at eliminating undesirable astrocytic differentiation for nervous system therapies.

In this respect, our group investigated the ability of protein-derived nanofiber meshes to affect neuronal development. Previously, we interrogated the bioactivity of electrospun nanofibers from laminin isolated from the murine EHS tumor [10,11]. While these fibers were ideal for neuronal outgrowth applications such as peripheral nerve transection injuries, laminin is a difficult protein to isolate and yields are typically low. The isolation process can be modified to instead produce higher yields of whole BM; this process is used commercially to isolate Matrigel (BD Biosciences) and other similar products (e.g. Stemgel, Stemgent, Inc.) using DMEM. We have modified the protocol so the end product is dissolved in distilled water, which allows for simple lyophilization to remove the liquid component to obtain the powder form of protein for solubilization and electrospinning following standard protocols. Utilizing this same process with commercially available BM materials would leave a considerable salt component and the phenol red coloring often added to DMEM in the electrospinning solution, thereby modifying the initial BM solution content and limiting its ability to hold charge and form chain entanglements required for successful fiber formation [34]. Our isolation method is thus superior for electrospinning nanofibers, though commercial versions of this material remain ideal for heat gel formation.

De Guzman *et al*. have recently described the electrospinning of commercial Matrigel preparations into nanofibers; however, their processes required significant modification of the solvent system to achieve fibers [35]. Our methods achieve nanoscale dimensions (mean fiber diameters around 100nm) and maintain the ability to modify the parameters during the electrospinning process to cause specific, reproducible morphological changes in the resultant nanofiber mesh. This control over fiber diameter and morphology provides the ability to tune the mesh characteristics to a specific application.

Electrospun proteins often undergo significant swelling, sufficient to obstruct pores and change the surface structure to microscale (>1,000nm) rather than nanoscale. With some proteins, hydration in aqueous media can result in complete dissolution of the mesh without prior use of harsh chemical crosslinkers [23]. As we demonstrated previously with laminin nanofibers [10], our RBM nanofibers do not swell to above 150nm in diameter. Maintenance of nanoscale fiber diameters and fibrous shape is critical to providing BM-mimetic substrates for culture.

While RBM may be sufficient to replicate the basement membrane for any regenerative medicine application, our focus in these studies was to establish its functionality as a substrate for peripheral nerve outgrowth. Further studies will continue to explore the attachment capacity and neurite-promoting activity of this mesh with other cell types. We expect this substrate to be useful for other tissue engineering applications due to its BM-mimetic structure and composition.

Although RBM nanofibers do alleviate some of the cost issues associated with laminin nanofibers, we sought to make this technology more accessible, as well as to improve repeatability and mechanical stability of the fibers to increase the chances for successful clinical translation of this substrate as a tissue engineered scaffold. Blending RBM with PCL provides these benefits as PCL is relatively inexpensive, is already approved by the FDA for use in various biomedical applications, and many groups have had success electrospinning this synthetic polymer. PCL maintains its fibrous morphology well in culture conditions and has a relatively slow degradation rate, making it ideal as a scaffold for peripheral nerve injuries, which may take many months to heal. The RBM-PCL blend nanofibers we fabricated demonstrated desired physical properties such as fiber diameter and morphology, as well as bioactivity in terms of attachment and neurite outgrowth, similar to pure RBM nanofibers. Both PC12 cells and primary neurons isolated from DRG showed characteristic neurite extension on blend nanofibers.

To further our pursuit of longer process extension for peripheral nerve regeneration, we fabricated aligned RBM-PCL blend nanofibers. The aligned morphology of our nanofibers promoted and directed neurite outgrowth. Other groups have shown consistent aspect ratio changes in multiple cell types on aligned nanofibers, and we saw similar effects on PC12 cells with our RBM-PCL blend aligned nanofibers.

In conclusion, we have successfully fabricated nanofibers consisting of single and whole BM components, as well as RBM-PCL blend nanofibers in both random and aligned orientations. Laminin-blend nanofibers have the potential to maintain undifferentiated human embryonic stem cells for longer durations between passages without the xenogenic byproducts of a mouse feeder layer. RBM fibers show promise as a substrate for cell adhesion and aligned RBM-PCL blend fibers may be ideal for applications where directional outgrowth is desired such as peripheral nerve regeneration or tendon repair. We expect these materials to prove useful in a variety of regenerative medicine applications as both their composition and structure closely mimic that of native basement membrane.

Acknowledgments

References

1. Abrams GA, Schaus SS, Goodman SL, Nealey PF, Murphy CJ. Nanoscale topography of the corneal epithelial basement membrane and Descemet's membrane of the human. Cornea. 2000; 19(1):57–64. [PubMed: 10632010]

2. Beachley V, Wen X. Polymer nanofibrous structures: Fabrication, biofunctionalization, and cell interactions. Progress in Polymer Science. 2010; 35:868–892. [PubMed: 20582161]

3. Flemming RG, Murphy CJ, Abrams GA, Goodman SL, Nealy PF. Effects of synthetic micro- and nano-structured surfaces on cell behavior. Biomaterials. 1999; 20(6):573–588. [PubMed: 10213360]

4. Lee CH, Shin HJ, Cho IH, Kang YM, Kim IA, Park KD, et al. Nanofiber alignment and direction of mechanical strain affect the ECM production of human ACL fibroblast. Biomaterials. 2005; 26(11): 1261–1270. [PubMed: 15475056]

5. Mo XM, Xu CY, Kotaki M, Ramakrishna S. Electrospun P(LLA-CL) nanofiber: a biomimetic extracellular matrix for smooth muscle cell and endothelial cell proliferation. Biomaterials. 2004; 25:1883–1890. [PubMed: 14738852]

6. Yeung T, George PC, Flanagan LA, Marg B, Ortiz M, Funaki M, et al. Effects of substrate stiffness on cell morphology, cytoskeletal structure, and adhesion. Cytoskeleton. 2005; 60(1):23–34.

7. Loesberg WA, Riet J, Van Delft FCMJM, Schon P, Figdor CG, Speller S, et al. The threshold at which substrate nanogroove dimensions may influence fibroblast alignment and adhesion. Biomaterials. 2007; 28(27):3944–3951. [PubMed: 17576010]

8. O'Brien FJ, Harley BA, Yannas IV, Gibson LJ. The effect of pore size on cell adhesion in collagen-GAG scaffolds. Biomaterials. 2005; 26(4):433–441. [PubMed: 15275817]

9. Scheppke L, Murphy EA, Zarpellon A, Hofmann JJ, Merkulova A, Shields DS, Weis SM, Byzova TV, Ruggeri ZM, Iruela-Arispe ML, Cheresh DA. Notch promotes vascular maturation by inducing integrin-mediated smooth muscle cell adhesion to the endothelial basement membrane. Blood. 2012; 119(9):2149–2158. [PubMed: 22134168]

10. Neal RA, McClugage SG, Link MC, Sefcik LS, Ogle RC, Botchwey EA. Laminin nanofiber meshes that mimic morphological properties and bioactivity of basement membranes. Tissue Engineering Part C:Methods. 2009; 15(1):11–21. [PubMed: 18844601]

11. Neal RA, Tholpady SS, Foley PL, Swami N, Ogle RC, Botchwey EA. Alignment and composition of laminin-polycaprolactone nanofiber blends enhance peripheral nerve regeneration. Journal of Biomedical Materials. In press; Part A

12. Tinois E, Tiollier J, Gaucherand M, Dumas H, Tardy M, Thivolet J. *In vitro* and post-transplantation differentiation of human keratinocytes grown on the human type IV collagen film of a bilayered dermal substitute. Experimental Cell Research. 1991; 193(2):310–319. [PubMed: 2004647]

13. Johnson G, Moore SW. Identification of a structural site on acetylcholinesterase that promotes neurite outgrowth and binds laminin-1 and collagen IV. Biochemical and Biophysical Research Communications. 2004; 319(2):448–455. [PubMed: 15178427]

14. Yap WT, Salvay DM, Silliman MA, Zhang X, Bannon ZG, Kaufman DB, Lowe W, Shea LD. Collagen IV-modified scaffolds improve islet survival and function and reduce time to euglycemia. Tissue Engineering A. 2013 epub ahead of print.

15. Martin MJ, Muotri A, Gage F, Varki A. Human embryonic stem cells express immunogenic nonhuman sialic acid. Nature Medicine. 2005; 11(2):228–232.

16. Cho M, Lee EJ, Nam H, Yang JK, Cho J, Lim JM, et al. Human feeder layer system derived from umbilical cord stromal cells for human embryonic stem cells. Fertil Steril. 2010; 93(8):2525–2531. [PubMed: 20403597]

17. Unger C, Felldin U, Nordenskjold A, Dilber MS, Hovatta O. Derivation of human skin fibroblast lines for feeder cells of human embryonic stem cells. Curr Protoc Stem Cell Biol. 2008; Chapter 1(Unit iC):7. [PubMed: 18770630]

18. Lai Y, Sun Y, Skinner CM, Son EL, Lu Z, Tuan RS, Jilka RL, Ling J, Chen XD. Reconstitution of marrow-derived extracellular matrix ex vivo: A robust culture system expanding large-scale highly functional human mesenchymal stem cells. Stem Cells and Development. 2010; 19(7):1095–1107. [PubMed: 19737070]

19. Benton G, Kleinman HK, George J, Amaoutova I. Multiple uses of basement membrane-like matrix (BME/Matrigel) *in vitro* and in vivo with cancer cells. Int.J. Cancer. 2011; 128:1751–1757. [PubMed: 21344372]

20. Kleinman HK, McGarvey ML, Liotta LA, Robey PG, Tryggvason K, Martin GR. Isolation and characterization of type IV procollagen, laminin and heparin sulfate proteoglycan from the EHS sarcoma. Biochemistry. 1982; 21:6188. [PubMed: 6217835]

21. Kleinman HK, McGarvey ML, Hassel JR, Martin GR. Formation of supramolecular complex is involved in the reconstitution of basement membrane components. Biochemistry. 1983; 22:4969. [PubMed: 6227336]

22. Kleinman HK. Preparation of basement membrane components from EHS tumors. Current Protocols in Cell Biology. 2001; 10(Unit 10.2)

23. Rho KS, Jeong L, Lee G, Seo BM, Park YJ, Hong SD, et al. Electrospinning of collagen nanofibers: effects on the behavior of normal human keratinocytes and early-stage wound healing. Biomaterials. 2006; 27:1452. [PubMed: 16143390]

24. Li D, Wang YL, Xia YN. Electrospinning of polymeric and ceramic nanofibers as uniaxially aligned arrays. Nano Letters. 2003; 3(8):1167–1171.

25. Kakade MV, Givens S, Gardner K, Lee KH, Chase DB, Rabolt JF. Electric field induced orientation of polymer chains in macroscopically aligned electrospun polymer nanofibers. J Am Chem Soc. 2007; 129(10):2777–2782. [PubMed: 17302411]

26. Chaurey V, Chiang P, Polanco C, Su Y, Chou C, Swami N. Interplay of electrical forces for alignment of sub-100 nm electrospun nanofibers at insulator gap collectors. Langmuir. 2010; 26(24):19022–19026. [PubMed: 21082824]

27. Xie J, MacEwan MR, Schwartz AG, Xia Y. Electrospun nanofibers for neural tissue engineering. Nanoscale. 2010; 2:35–44. [PubMed: 20648362]

28. Subramanian A, Krishnan UM, Sethuraman S. Fabrication of uniaxially aligned 3D electrospun scaffolds for neural regeneration. Biomed. Mater. 2011; 6(2):025004. [PubMed: 21301055]

29. Rodin S, Domogatskaya A, Strom S, Hansson EM, Chien KR, Inzunza J, et al. Long-term self-renewal of human pluripotent stem cells on human recombinant laminin-511. Nat Biotechnology. 2010; 28(6):611–615.

30. Xie J, Willerth SM, Li X, Macewan MR, Rader A, Sakiyama-Elbert SE, et al. The differentiation of embryonic stem cells seeded on electrospun nanofibers into neural lineages. Biomaterials. 2009; 30(3):354–362. [PubMed: 18930315]

31. Lim SH, Liu XY, Song H, Yarema KJ, Mao HQ. The effect of nanofiber-guided cell alignment on the preferential differentiation of neural stem cells. Biomaterials. 2010; 31:9031–9039. [PubMed: 20797783]

32. Cho YI, Choi JS, Jeong SY, Yoo HS. Nerve growth factor (NGF)-conjugated electrospun nanostructures with topographical cues for neuronal differentiation of mesenchymal stem cells. Acta Biomaterialia. 2010; 6:4725–4733. [PubMed: 20601229]

33. Prabhakaran MP, Jayarama RV, Ramakrishna S. Mesenchymal stem cell differentiation to neuronal cells on electrospun nanofibrous substrates for nerve tissue engineering. Biomaterials. 2009; 30(28):4996–5003. [PubMed: 19539369]

34. Nie H, He A, Zheng J, Xu S, Li J, Han CC. Effects of chain conformation and entanglement on the electrospinning of pure alginate. Biomacromolecules. 2008 May; 9(5):1362–1365. [PubMed: 18433165]

35. de Guzman RC, Loeb JA, VandeVord PJ. Electrospinning of matrigel to deposit a basal lamina-like nanofiber surface. J Biomater Sci Polym Ed. 2010; 21(8–9):1081–1101. [PubMed: 20507710]
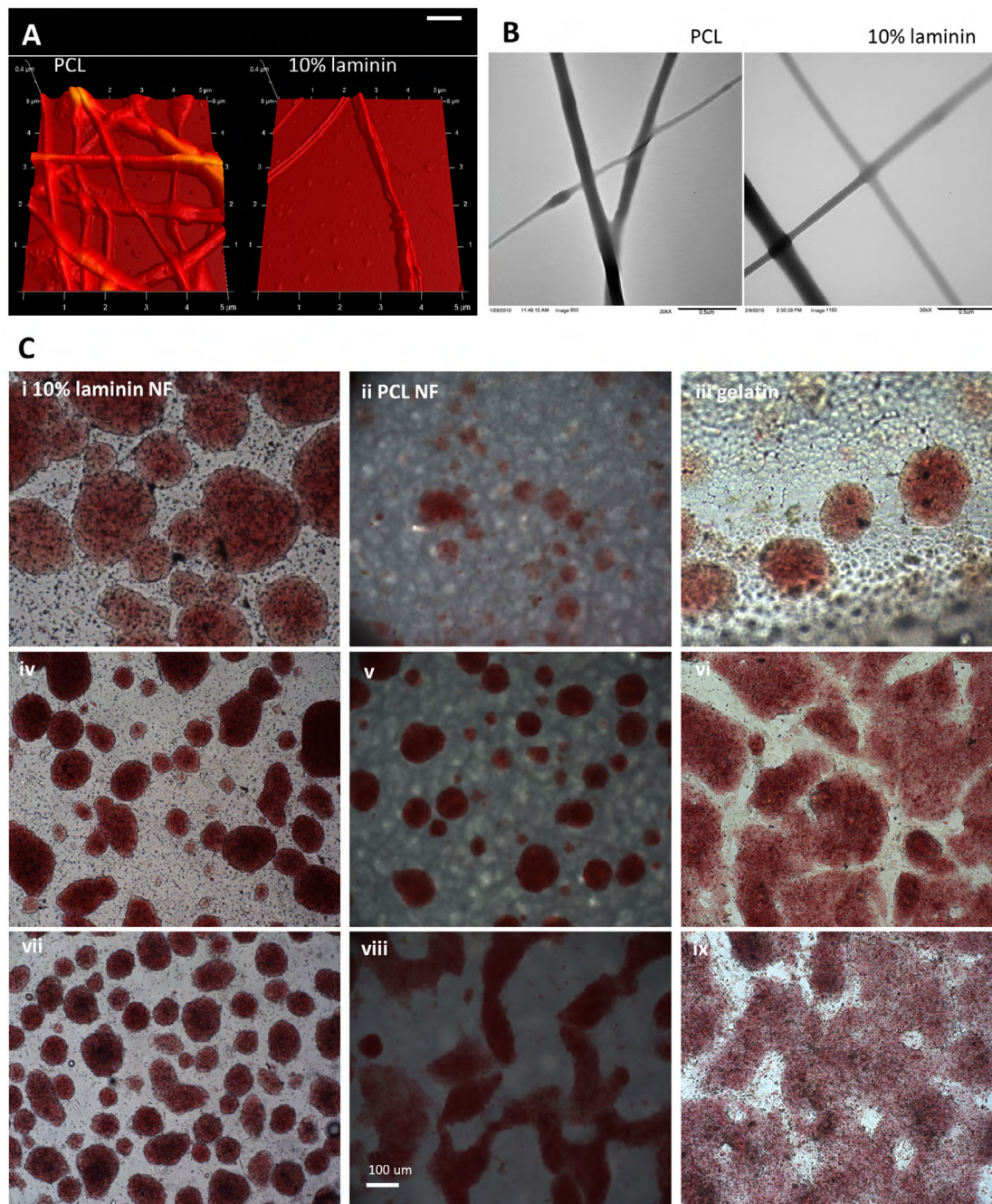
Figure 1.
Mouse ES cells maintain stemness on laminin nanofibers. A) Atomic force microscopy and B) transmission electron microscopy images of PCL nanofibers and 10% laminin, 90% PCL nanofibers. C) Mouse ES cells cultured on 10% laminin nanofibers (column 1), polycaprolactone nanofibers (column 2), gelatin (column 3) without passage for 2 days (row 1), 4 days (row 2), and 8 days (row 3). Cells are stained with alkaline phosphatase to distinguish undifferentiated cells (red) and differentiated cells (yellow). Gelatin groups begin to show yellow staining at 8 days, as well as altered morphology. After 8 days without passage, the

ES cells cultured on laminin nanofibers are better able to maintain their colony formation, which is necessary to remain undifferentiated. Image axes in (A) are 5μm × 5μm × 0.4μm. Scale bar in (B) = 0.5μm. Scale bar in (C) = 100μm.
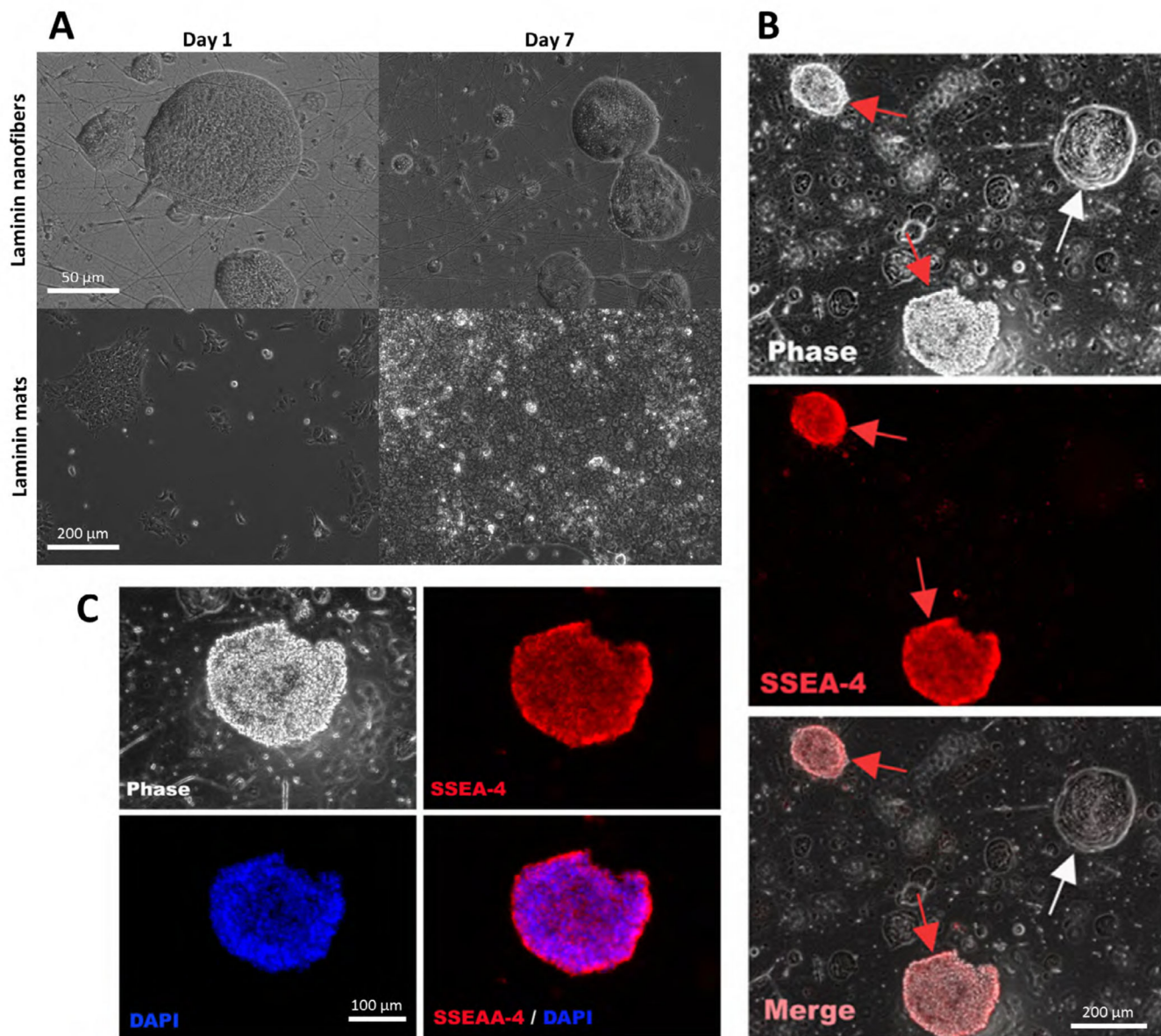
Figure 2.
Human embryonic stem cells maintain undifferentiated state on laminin nanofibers. A) SEM micrographs of human embryonic stem cells (huES16) cultured on laminin nanofibers (top row) on Day 1 and Day 7, and huES cultured on laminin films (bottom row) on Day 1 and Day 7. B) huES16 human embryonic stem cells grown in feeder-free culture on laminin nanofibers. SSEA-4 is a stemness marker which indicates undifferentiated cells. On laminin nanofibers, the ES cells remain about 75% undifferentiated, and take on the unique morphology shown here. C) Magnified region of (B). SSEA-4, DAPI, and overlay images shown. Scale bar in (A) = 50μm, 200μm. Scale bar in (B) = 200μm. Scale bar in (C) = 100μm.
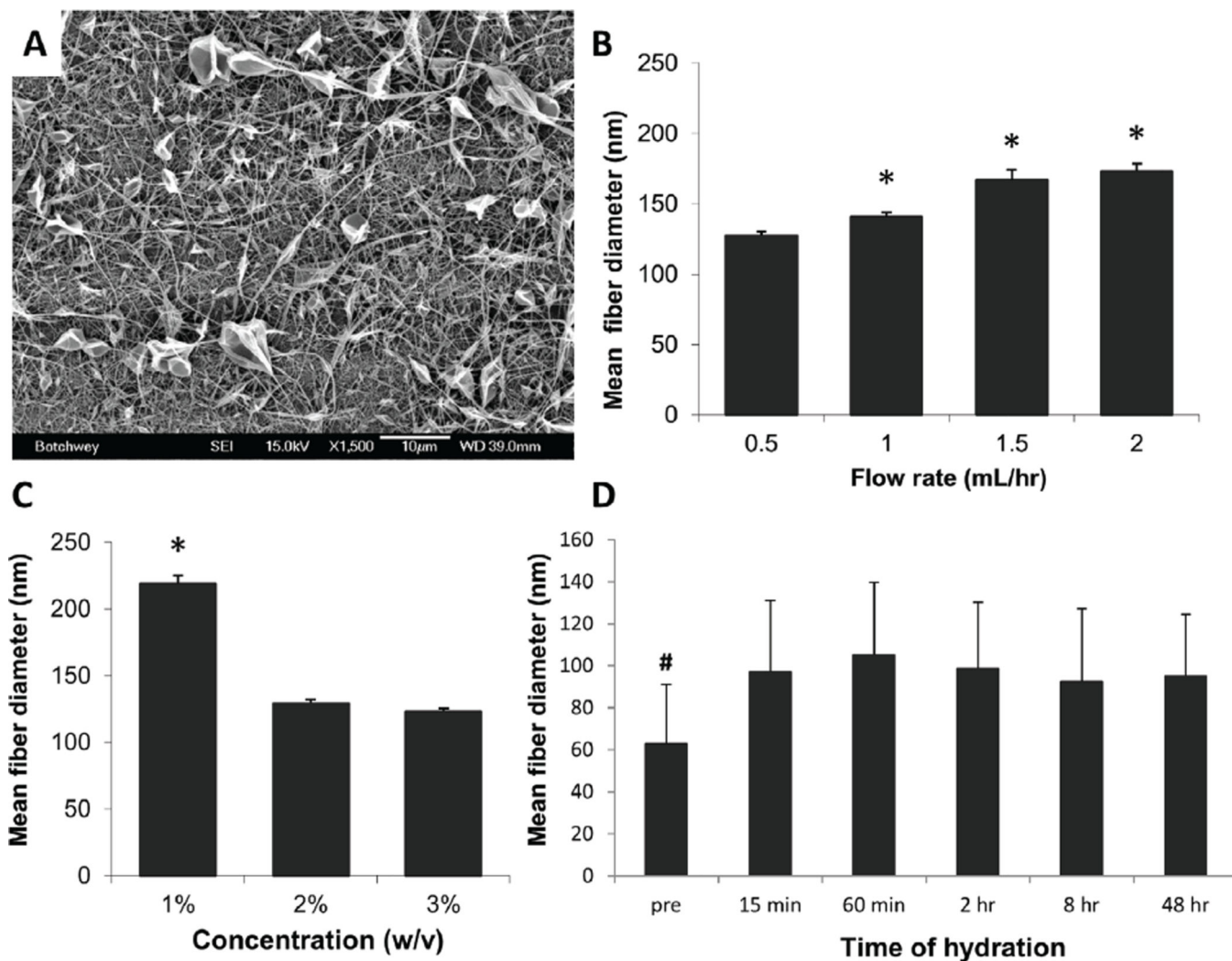
Figure 3.
Parametric manipulations exert control over RBM fiber diameter. (A) Representative scanning electron micrograph indicating successful fiber formation at 3% (w/v) initial concentration, 1.5mL/hr flow rate. Parametric manipulations, especially with flow rate (B) and concentration (C) exert changes in fiber diameter. Error bars display standard deviation. All parameter sets which include 1% (w/v) concentration are included in that bar, regardless of the other parameters. (D) RBM nanofibers resist morphology changes with hydration. Graph depicts percent swelling of fibers, which remains consistent at about 50% swelling over 48 hours, though fibrous morphology is maintained. Fiber diameter is significantly greater at all hydrated time points than fibers before hydration (pre), but no significant difference was found among hydration time points. Significance is denoted as * P < 0.01, and indicates significance over all other bars within the graph. # indicates P < 0.05 for difference between pre and all hydrated groups. Scale bar = 10μm.
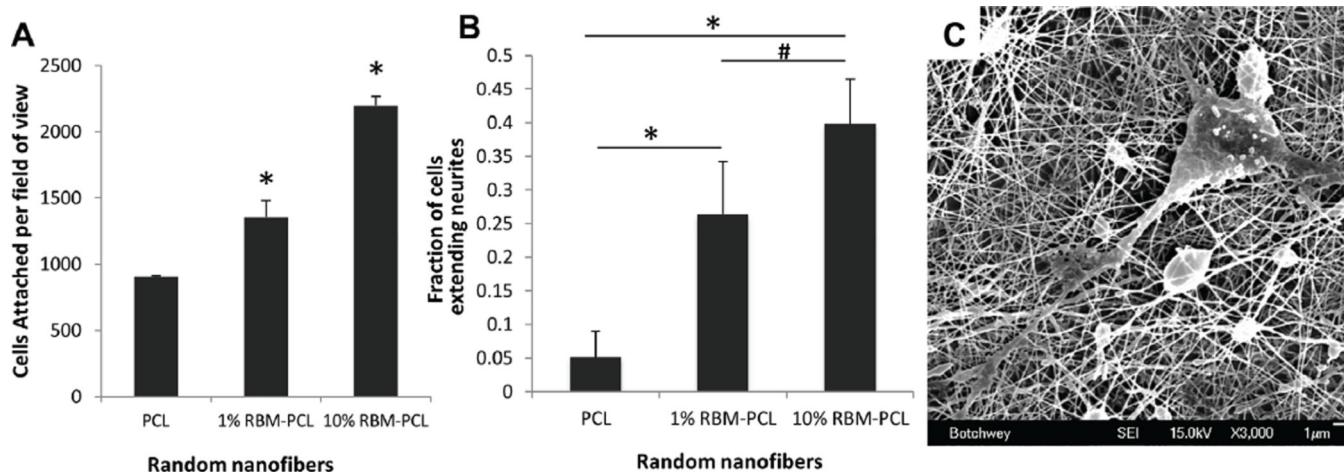
Figure 4.
PC12 cell attachment and neurite extension. (A) PC12 cells seeded on varying concentrations of RBM-PCL random nanofibers. ImageJ's area analysis tool was used to calculate the number of attached cells per field of view after 2hr incubation. Attachment on 10% RBM-PCL nanofibers was significantly greater than all other groups, and attachment on 1% RBM-PCL nanofibers was significantly greater than that on PCL. (B) Neurite extension of PC12 cells seeded on varying concentrations of RBM-PCL random nanofibers. After 5 DIV, cells with extensions greater than twice the length of their diameter were considered to be neurite-extending. The percentage of neurite-extending cells on 1% and 10% RBM-PCL nanofibers was significantly greater than that on PCL nanofibers. Extension was also significant between the RBM-PCL groups. Error bars display standard deviation. Significance is denoted as * $P < 0.001$ and # $P < 0.015$. (C) Representative SEM micrograph illustrating process extensions of primary neuron dissociated from murine DRG on 10% RBM-PCL nanofibers. Scale bar = 1μm.
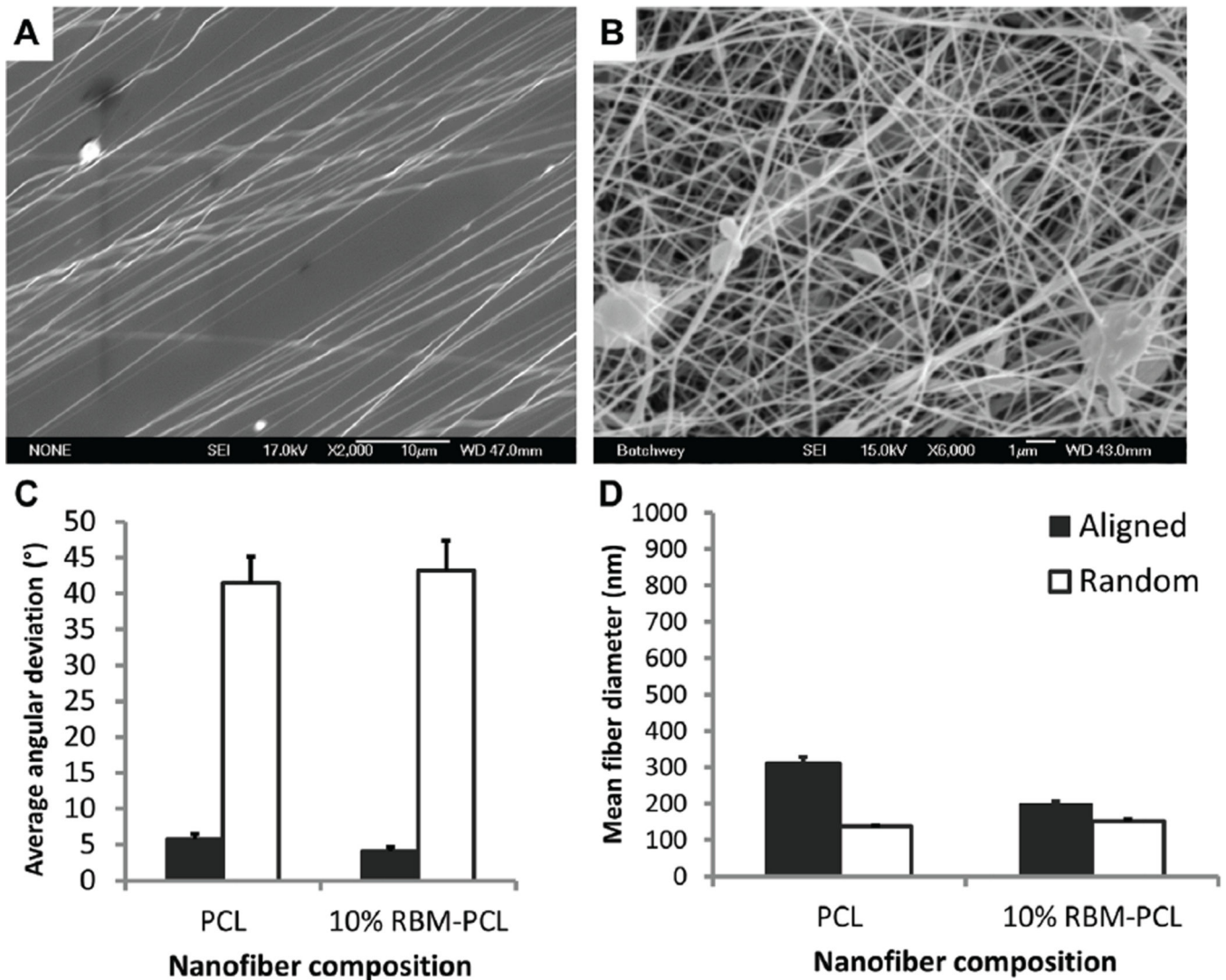
Figure 5.
Parametric manipulations exert control over fiber orientation. SEM micrographs of (A) aligned and (B) randomly oriented 10% RBM-PCL nanofibers. Angular deviations were measured relative to an axis of alignment. (C) Average angular deviation for both aligned PCL and 10% RBM-PCL was below 6 degrees, suggesting a high degree of alignment compared to randomly oriented nanofibers. (D) Fiber diameters of aligned and random substrates fell within the 30–400 nm range typically seen in basement membrane morphology. All error bars represent standard error. Scale bar in (A) = 10μm. Scale bar in (B) = 1μm.
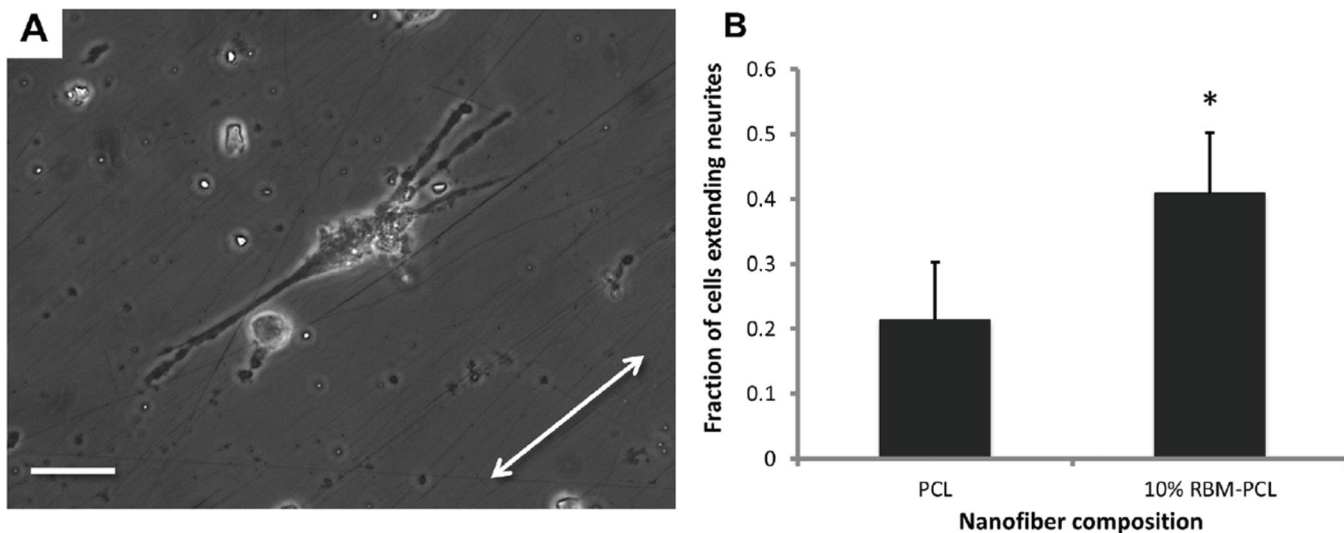
Figure 6.
Neurite extension on aligned nanofibers. (A) PC12 cells seeded on 10% RBM-PCL nanofibers show process extension along aligned nanofiber substrate. Arrow indicates nanofiber axis. (B) After 5 DIV, cells with extensions greater than twice the length of their diameter were considered to be neurite-extending. The percentage of neurite-extending cells on 10% RBM-PCL nanofibers was significantly greater than that on PCL nanofibers (*, $P = 0.004$). Error bars represent standard deviation. Scale bar = 50μm.